Advanced Energy Conversion Materials
http://ojs.wiserpub.com/index.php/AECM/

UNIVERSAL WISER PUBLISHER

Research Article

Conversion of Heat into Electricity Through Natural Convection of a Single-Phase Liquid Metal in a Closed Loop with a Magnetic Field

Andrea Di Vita[1*], Yuval Baryossef[2]

[1]Department of Civil, Chemical and Environmental Engineering, DICCA University of Genoa, Genoa, Italy
[2]Noga Photonics Ltd, Jaffa, Israel
E-mail: Andrea.DiVita@ansaldoenergia.com

Received: 11 May 2023; **Revised:** 31 July 2023; **Accepted:** 4 August 2023

Abstract: Conventional waste heat recovery systems usually require water (e.g. to supply steam for a turbine) and imply the wearing of moving parts, to the detriment of usability in case of drought and/or in the long term. Unconventional approaches (thermoacoustic and thermoelectric conversion of heat into electricity) overcome these obstacles, but their utilization for multi Kilowatt (KW) electric power in an industrial environment is jeopardized either by large working pressure, excessive noise, the need for cooling systems or huge magnetic fields. Welander and Erhard et al. discuss the existence and the stability of steady-state convection driven by an applied temperature gradient of a fluid circulating in a tube that forms a vertical, closed loop. Convection ensures the spontaneous conversion of heat into mechanical energy through competing buoyancy, drag and heat conduction between the fluid and the walls of the tube. Crucially, their results do not depend on the nature of the drag. If the working is an electrical conductor and a magnetic field is applied, the impact of the resulting Lorenz force acts as a drag on the motion of the fluid just like viscosity; the viscous and the magnetic drag are dealt with on an equal basis. The magnetic drag transforms the mechanical energy of the convective motion of the fluid into electric energy. Since convection is driven by a temperature gradient, spontaneous, water-free conversion of heat into electricity occurs with no moving part at atmospheric pressure. Such conversion is suitable for the purposes of waste heat recovery. As an example, let a 1-cm-radius tube filled Galinstan™ (a commercially available, atoxic liquid metal alloy) be rolled up in a double helix wrapped around a 30-m-tall, 3-m-radius chimney located above a furnace. If there is a 350 K temperature difference between the bottom of the tube (near the furnace) and the top, and if permanent magnets located on the tube provide a 0.017 T magnetic field, then conservative estimates show that we obtain 2 KW DC electric power with efficiency > 2.1%. This lower bound suggests that our system is competitive with thermoacoustic and thermoelectric conversion.

***Keywords*:** waste heat recovery, convection, magnetohydrodynamics, liquid metal

Nomenclature

A	cross section
$\boldsymbol{B}$	magnetic field
c_p	specific heat at const. press. per unit mass
D	hydraulic diameter

DOI: https://doi.org/10.37256/aecm.4220233021

f_D	*D'*Arcy factor
f_N	numerical coefficient in Colebrook-White equation
$\boldsymbol{F}$	drag force density
g	intensity of gravitational acceleration
h	wall-fluid heat exchange coefficient
H	modified squared Hartmann number
H	pitch
k	1/(wall-fluid heat exchange time-constant)
L	total length of the loop
MHD	magnetohydrodynamic
$\dot{m}$	mass flow
Nu	Nusselt number
p	pressure
Pr	Prandtl number
r	helix radius
R	1/(drag time-scale)
R_{Lorenz}	magnetic contribution to R
R_{visc}	viscous contribution to R
R_0	$D/2$
Re	Reynolds number
Re_m	magnetic Reynolds number
s	arc length
$\boldsymbol{s}$	unit tangent vector
dS_{lat}	infinitesimal lateral surface
t	time
t_H	heat diffusion timescale
t_{loop}	time required by one complete loop
t_M	momentum diffusion timescale
T	fluid temperature
TA	thermoacoustic
TE	thermoelectric
T_0	wall temperature
v_s	$\boldsymbol{v} \cdot \boldsymbol{s}$
$\boldsymbol{v}$	velocity
V	vertical dimension
W	mechanical power
W_{grid}	power available to the load
W_{Joule}	power dissipated by Joule heating
W_{Lorenz}	electromagnetic power
W_{th}	amount of heat exchanged per unit time
W_{visc}	power dissipated by viscosity
$\boldsymbol{z}$	vertical unit vector
α	thermal expansion coefficient
α_E	modified Prandtl number
β_E	modified Rayleigh number
ΔH	equivalent pressure drop
Δs	length of arc-like connection
$\Delta\Theta$	max. jump of T
η	efficiency
η_L	lower bound on η

κ	thermal conductivity
μ	dynamic viscosity
μ_0	magnetic permittivity of vacuum
ν	kinematic viscosity
ρ	mass density
ρ_0	reference value of ρ
σ	electrical conductivity

1. The problem

With the rising concern regarding global warming, waste heat recovery is of fundamental interest when it comes to reducing fuel consumption, lower harmful emissions, and improving production efficiency. to generate electricity out of waste heat, most approaches presently require the availability of water as a working fluid (possibly as steam) and rely on mechanical moving parts (e.g., turbines). The former may be a problem in the (all too likely) case of drought; the latter raises concerns about long-term maintenance, due to unavoidable mechanical wearing [1].

A list of today's (2023) most widely investigated alternative approaches to waste heat recovery and conversion into electricity includes Thermoelectric (TE), Thermoacoustic (TA) and Magnetohydrodynamic (MHD) conversion. Unfortunately, none of them seem yet to be profitable.

Significant drawbacks affect the first two when it comes to electric power of industrial interest (say, > 1 KW). As for TE, where a solid-state device converts heat flowing across the system (this flux being related to temperature difference inside the device) directly into electrical energy through the Seebeck effect, the (typically low) thermal conductivity of TE materials facilitates local overheating, which in turn affects the electrical resistivity and spoils therefore the optimum impedance matching between the source and the grid. Additional, dedicated, cooling systems prevent such overheating like in automotive applications; but these systems require water. Heat-to-electricity efficiency η is in the range of 1.3%/6% [2]; it overcomes 20% only when coupled to photovoltaic devices - of course, in daylight only [3]. As for thermoacoustics, where heat flux is transformed into acoustic energy and its acoustic energy is in turn transformed into electric energy through some mechanical or magnetic device, the amplitude of the sound wave becomes so large that the mechanical integrity of the system is at stake when it comes to electric power >> 10 KW. Beyond noise, further problems are the huge values of the magnetic field (≈ O(1) T - see Table 1 of [4]) and of the working pressure involved (≈ 5 bar - see Sec. 7.2 of [5]), which may lead to significant (magneto)mechanical stress; moreover, magnets may require a dedicated power supply. The efficiency is the product of the heat-to-mechanical conversion energy (sound) efficiency and of sound-electric conversion efficiency; typical optimum values are 0.28 times the Carnot efficiency and 40% respectively so that η = 0.11 times the Carnot efficiency. If the highest temperature of the system is three times the lowest one, so that Carnot efficiency is 33%, then η = 3.6%. Such low value is due to unavoidable entropy production due to irreversible heat conduction - see Sec. 4c and Figure 28 of [6]. Admittedly, a record efficiency η = 19.8% has been claimed [7] - but with 40 bar working pressure.

The remaining option, MHD, allows the transformation of the kinetic energy of a fluid that has high electrical conductivity and is immersed in a magnetic field [8]. If the electrically conducting fluid flows in a tube at constant velocity across the field lines of a constant magnetic field, then Direct Current (DC) electric current is collected on the walls of the tube. MHD does the job with no overheating (as the heat is advected by the fluid) unlike TE and silently (unlike TA), provided that an effective system of transformation of heat into the kinetic energy of the fluid is available. As a matter of principle at least, the only upper bound on the achievable electric power is set by the amount of kinetic energy of the fluid. As for waste heat recovery, the weak point of MHD is precisely the required conversion of heat - say, the internal energy of the fluid - into mechanical energy. If the fluid is either plasma or gas, then it is compressible, and a Venturi tube does the job. But then, plasmas are plagued by instabilities, while gases have negligible electrical conductivity; to raise the latter, they are inseminated with ions, and the process raises problems of pollution and consumption of materials. If the fluid is a liquid, then its electrical conductivity σ may be far from negligible (from 5 S/m of seawater to 10^6 S/m in mercury). But liquids are basically incompressible, and Venturi is of no use.

Nature seems to offer a solution. If the difference of temperature between the hottest and the coldest point in the

fluid is large enough and is kept constant by the external world, then convection spontaneously transforms heat flowing across the fluid into mechanical energy even at atmospheric pressure. This is just the well-known working principle of the thermosyphon, *a circulating fluid system whose motion is caused by density differences in a body force field that result from heat transfer* [9]. It works even if the fluid is electrically conductive, as it is well-known e.g. in geophysics. If σ is large enough (>> 1 S/m), then we show that conversion of a significant fraction of the resulting kinetic energy of the fluid into electric energy occurs provided that the system is immersed in a moderate magnetic field (<< 1 T). Admittedly, the fluid velocity associated with convection may be relatively low (< 1 m/s), so that the density of electric energy obtained through this process is also low. But energy is an additive quantity; if the fluid fills completely in a tube forming a long, closed loop with constant cross-section and flows across it because of convection, then the total electric energy output increases with increasing tube length and can be far from negligible. The fact that a unit length of the tube collects only a small amount of electric energy is in fact highly desirable as it prevents the formation of undesirable voltage peaks along the loop. Given the desired value of electric power, setting up a long tube filled with fluid that forms a closed loop (possibly rolled up like the copper wire of a solenoid) and is immersed in a magnetic field is much simpler than setting up a system of steam turbines and the like, as no solid moving parts are involved. Permanent magnets provide the required magnetic field with no need for a power supply. Moderate magnetic field and atmospheric working pressure rule out excessive mechanical stresses. If no phase transition and no electrochemical deposition of solid residue on the tube wall occurs, then we may safely take the thermophysical properties of the working fluid as uniform in the loop. The constant cross-section of the tube ensures that the fluid velocity is uniform along the tube so that a smooth MHD conversion process occurs uniformly along the loop.

This MHD conversion relies on large values of σ and works even for uniform magnetic fields. The process differs sharply from thermomagnetic convection [10, 11], a process relevant to magnetizable nanofluids [12-15] where the magnetic force acting of the fluid is a linear combination of terms that are proportional to the gradients of the components of the magnetic field - see equation (13) of [11] - and does not depend on σ (which, by the way, is ≈ 0.1 S/m in some ferrofluids [16]).

The aim of the present work is twofold: a) to discuss the natural convection of an electrically conducting fluid in a closed, long loop with a given difference $\Delta\Theta$ of temperature between the hottest and the coldest point of the loop; b) to apply the results of this discussion to MHD conversion when a magnetic field $\boldsymbol{B}$ is applied and the fluid is electrically conducting. We invoke the familiar Boussinesq approximation and limit ourselves to the case of constant $\Delta\Theta$, having in mind the static conversion of energy. Moreover, we assume that the fluid is a chemically pure substance; as for electrically conducting liquids, this means liquid metals and excludes solutions like seawater. Consequently, we need no bother with electrolysis and other chemical processes which can lead to unwanted deposition of material on the tube walls. Furthermore, we assume that the temperature always remains within a range where there is only one liquid phase, for simplicity. The buoyancy force is counteracted by a drag force: the two forces are equal and opposite in a steady state. Finally, we assume also that the length of the loop is >> the hydraulic diameter of the tube. This inequality has two consequences. Firstly, the exchange of heat between the fluid and the wall of the tube rules heat conduction. Secondly, the impact on the viscous drag of the viscous forces acting among different fluid parcels in the fluid bulk is negligible in comparison with the impact of the friction of the fluid with the wall; the only fluid motion considered is parallel to the tube.

To show that a stable, steady convection exists and allows effective MHD conversion of thermal into electric energy we take advantage of the results of [17] and [18]. The former describes the convection of a single-phase incompressible fluid in a closed loop. Even if the author focuses his attention on the onset of oscillatory instabilities (due to the overplay of buoyancy, drag and heat transport, as previously stated also in [19] and [20]), his results are largely independent from the detailed description of the physical process underlying the drag. The same feature is shared by [18], which displays an extensive investigation (both linear and nonlinear) on the stability of a system that generalizes the loop of [17], and outlines the conditions for the existence and the stability of a steady state (envisaged also in [20]). Experiments [18, 21-23] confirm the findings of [18], even if with $\boldsymbol{B} = 0$. Since its results do not depend on what the drag is like, we apply it to an electrically conducting, viscous fluid in a closed loop where both viscosity and $\boldsymbol{B}$ contribute to the drag.

The paper is organized as follows. We discuss the model of [17] and [18] in Sec. 2. Steady states and their stability are investigated in Sec. 4. We discuss viscous and magnetic drag in Sec. 4. Useful formulas for numerical computation are derived in Sec. 6. A lower bound on the efficiency of the conversion of heat into electricity is computed in Sec. 7.

We discuss a practical example in Sec. 7, where we choose a commercially available metal liquid alloy, Galinstan™, as working fluid. Conclusions are drawn in Sec. 8.

2. The model

We take a narrow tube of a uniform cross-section of area $A = \pi R_0^2$, hydraulic diameter $D = 2\sqrt{A/\pi} = 2R_0$ and total length $L \gg R_0$. We form the tube into a closed loop made of 2 vertical, equally long branches with semicircular, arc-like connections of length $\Delta s \left(0 \le \Delta s \le \frac{L}{2} \right)$ at the top and at the bottom - see Figure 1 (Our results below are not affected if we drop the assumption of exactly vertical branches). We denote with s ($0 \le s \le L$) the arc length along the tube with unit vector $\boldsymbol{s}$, where $s = 0$ at the bottom and $s = \frac{L}{2}$ at the top. We identify the right branch $\frac{\Delta s}{2} \le s \le \frac{L}{2} - \frac{\Delta s}{2}$, the left branch $\frac{L}{2} + \frac{\Delta s}{2} \le s \le L - \frac{\Delta s}{2}$, the top arc-like section $\left(\frac{L}{2} - \frac{\Delta s}{2} \le s \le \frac{L}{2} + \frac{\Delta s}{2} \right)$ and the bottom arc-like section $\left(L - \frac{\Delta s}{2} \le s \le L,\ 0 \le s \le \frac{L}{2} \right)$. The tube is filled with incompressible, viscous, single-phase and (possibly) electrically conductive fluid. The tube walls are kept at a prescribed temperature T_0 that varies along the loop, i.e. $T_0 = T_0(s)$. The fluid is ruled by:

$$\nabla \cdot \boldsymbol{v} = 0 \tag{1}$$

$$\rho_0 = \frac{d\boldsymbol{v}}{dt} = -\nabla p - \rho g \boldsymbol{z} + \boldsymbol{F} \tag{2}$$

$$\rho = -\rho_0 \alpha T + \text{const.} \tag{3}$$

were we adopt Boussinesq approximation and g, $p = p(\rho_0, T)$, ρ, α, T, ρ_0, $\boldsymbol{z}$, $\boldsymbol{v}$ and $\boldsymbol{F}$ are the intensity of gravitational acceleration, the fluid pressure, mass density, thermal expansion coefficient and temperature, a reference value of the mass density ρ (taken e.g. at 300 K), the vertical unit vector and the drag force per unit volume respectively. Since $R_0 << L$, we write $t_M < t_{loop}$ where momentum diffusion over the cross section occurs in a time $t_M \equiv \frac{\rho R_0^2}{4\mu}$ (μ is the dynamic viscosity) and the time required for a complete turn around the loop is $t_{loop} \equiv \oint \frac{ds}{vs}$. Then, (1) implies $v_s \equiv \boldsymbol{v} \cdot \boldsymbol{s} = v_s(t)$, so that $t_{loop} = \frac{L}{v_s}$. Moreover, heat diffusion over the cross section occurs in a time $t_H \equiv \frac{\rho R_0^2 c_p}{4\kappa} = t_M Pr$ (κ thermal conductivity, c_p specific heat per unit mass at constant pressure, $Pr \equiv \frac{c_p \mu}{\kappa}$ Prandtl number). Since $R_0 << L$, we write $t_H < t_{loop}$. We also neglect the heat conduction within the fluid along the tube in comparison with the heat conduction between the fluid and the tube wall. Accordingly, we assume that T is uniform over each cross-section, i.e.: $T = T(s, t)$. We encompass the inequalities $t_M < t_{loop}$ and $t_H < t_{loop}$ in 1 self-consistency condition:

$$\frac{Re}{4} \frac{R_0}{L} \max(1, Pr) < 1 \tag{4}$$

($Re \equiv \frac{v_s R_0}{\nu}$ Reynolds number, $\nu \equiv \frac{\mu}{\rho_0}$ kinematic viscosity). We allow $\boldsymbol{F}$ to depend on both s and v_s and write $\boldsymbol{F} \cdot \boldsymbol{s} = \rho_0 R v_s$ where $R = R(s, v_s) > 0$ has the dimension of time^{-1}. According to (2) and (3), the fluid is driven by the buoyancy force and is retarded by a drag force. Dot product of both sides of (2) by $\boldsymbol{s}$ gives:

$$\rho_0 \frac{\partial v_s}{\partial t} = -\frac{\partial p}{\partial s} - \rho g \boldsymbol{z} \cdot \boldsymbol{s} + \rho_0 R v_s \tag{5}$$

regardless of the structure of R, i.e. of the detailed physical mechanism underlying $\boldsymbol{F}$. We describe convection as a 1D flow moving along the closed loop - i.e., $\boldsymbol{v} = v_s \boldsymbol{s}$ - and subjected to given heat sources and sinks along the path. The heat transfer to the fluid is assumed to be proportional to the difference between the local temperature T_0 of the wall and T:

$$\frac{dT}{dt} = \frac{\partial T}{\partial t} + v_s \frac{\partial T}{\partial s} = k(T_0 - T) \tag{6}$$

where $k = k(s, v_s) \geq 0$ has the dimension of time^{-1}. Note that (6) includes no bulk heating term; we shall discuss this point below. Once the geometry (i.e. the dependence of $\boldsymbol{z} \cdot \boldsymbol{s}$ on s), $T_0(s, t)$, $p = p(\rho_0, T)$, $R(s, v_s)$ and $k(s, v_s)$ are known, then (3), (5) and (6) provide $\rho(s, t)$, $v_s(t)$ and $T(s, t)$. Periodicity requires $T_0(s, t) = T_0(s + L, t)$, $T(s, t) = T(s + L, t)$ and $\rho(s, t) = \rho(s + L, t)$.

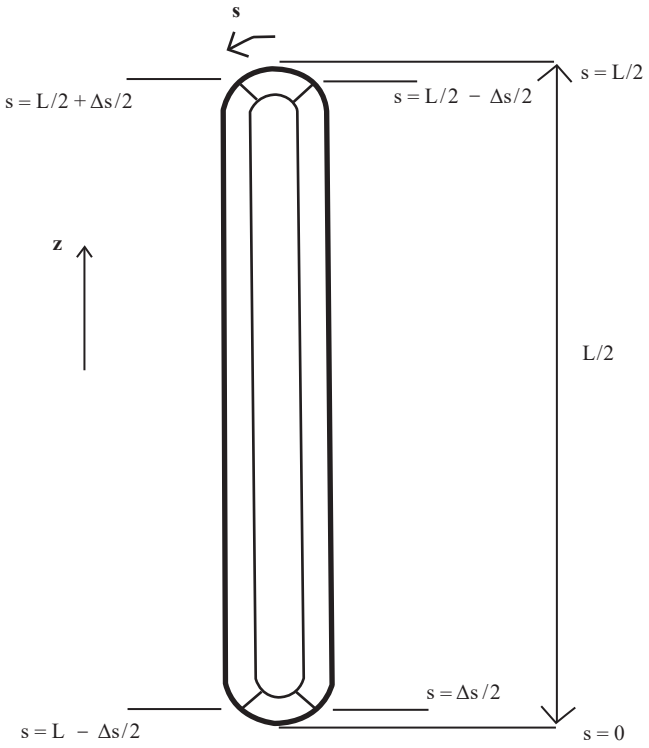

Figure 1. A narrow tube of total length L and hydraulic diameter $D << L$ forms a closed loop and is filled with fluid. The loop is made of two vertical branches with connections at the top and the bottom. The tube is symmetric with respect to the vertical. Both vertical branches are thermally insulated (k = 0). The length of each short connection is Δs. The temperature of the wall is kept at $-\frac{\Delta\Theta}{2}$ and $+\frac{\Delta\Theta}{2}$ at the arc-like connection at the top and the bottom respectively, where the wall temperature at half height $\left(s = \frac{1}{4},\ s = \frac{3L}{4}\right)$ is set to zero. Since $q > 0$, the vertical unit vector $\mathbf{z} \cdot \mathbf{s} = +1$ (-1) on the right (left) vertical branch. For the sake of clarity, both vertical branches displayed are straight; however, this is not required in our discussion

3. Steady states and their stability

Many authors discuss in detail the solutions of the system of equations (3), (5) and (6) in different cases [17, 18, 20-

23] and show that these solutions accurately describe experiments [18, 21-23]. Relaxation to a steady solution $\left(\frac{\partial}{\partial t} \equiv 0\right)$ is possible. Lack of convection in the relaxed state occurs for $v_s = 0$. This $v_s = 0$ steady state is stable whenever the ratio β_E of the buoyancy force and the drag force is < 1 [18]; we write down an explicit expression for β_E below. (Periodicity makes the contribution of p to β_E to vanish [17]). As $\beta_E > 1$, convection starts with constant $v_s \neq 0$. As for a detailed description of this case see [17] for k = const. > 0, $T_0(s) = T_0(s = 0)$, k = const. > 0, $T_0(s) = T_0(s = 0) - \Delta\Theta$ in the bottom and in the top arc-like section respectively, with $k = 0$ elsewhere and $\Delta s << L$ in both cases; see also [20] in a slightly different geometry. Here $\Delta\Theta$ is the maximum and the minimum value of T_0. At even larger values of β_E (or, equivalently, of the flow rate [17]) spontaneous oscillations occur [18] regardless of the fluid inertia [20].

As suggested in a seminal paper of [19], dissipation can destabilize the periodic motion up and down of a fluid in a gravitational field, like e.g. the convective motion of the fluid in our closed loop. In the words of [17], *as the flow rate is increased above the critical value there is one upper and one lower value of Rt_{loop} for which neutral oscillations occur; in the range between these the solutions are amplified*. Reliable steady conversion of heat into electricity requires that convection not only actually occurs, but that it is also stable. The analysis of [18] generalizes the analysis of [17] to the case $T_0(s) = T_0(L - s)$ (corresponding to symmetric heating of the fluid around $s = 0$) while dropping the assumption $\Delta s << L$. In both [17, 18] and [20], however, two processes rule the flow of energy across the system: heat conduction between the fluid and the wall - with typical timescale k^{-1} - and the drag along the tube - with typical timescale R^{-1}. According to (4), both processes are concerned with the interactions of the fluid particles with the wall of the tube, rather than with each other: accordingly, suitably modified definitions of Prandtl, Rayleigh and Hartmann number shall be at hand below. We discuss both processes to check stability.

As for heat conduction, heat exchange occurs across the lateral surface of the arc-like connection at the bottom with length Δs where $k \neq 0$ Within this connection, let us focus our attention on a sector of infinitesimal length ds. In this sector, the external world supplies the fluid with an amount $dW_{th} = h_W(T(s) - T_0(s))Ads$ of heat per unit time, where we compute the proportionality factor h_W [18] by recalling that with $dW_{th} = h(T(s) - T_0(s))dS_{lat}$ with h heat exchange coefficient and $dS_{lat} = 2\pi R_0 ds$; hence:

$$h_W = \frac{2h}{R_0} \tag{7}$$

Similar considerations apply to the arc at the top, where the heat flows towards the external world; numerical data do not change as far as h is the same. We apply both (6), (7) and the first principle of thermodynamics to our sector and write $\frac{2h}{R_0}(T(s) - T_0(s))Ads = h_W(T(s) - T_0(s))Ads = dW_{th} = \rho_0 c_p \frac{dT}{dt} Ads = \rho_0 c_p k(T(s) - T_0(s))Ads$. It follows that:

$$k = \frac{2h}{\rho_0 c_p R_0} \tag{8}$$

Moreover, equation (6) in steady state provides us with a reasonable estimate of v_s:

$$v_s = k\Delta s \tag{9}$$

Experimentally, both the flow rate ($\propto v_s$) [22] and Re [21, 22] are proportional to the heat flux ($\propto h \propto k$); moreover, our assumption of identical values of h both at the top and at the bottom arc-like connection agrees with the experimental observation that the value of the Nusselt number $Nu \equiv \frac{hR_0}{\kappa}$ is basically constant along the heated zone [23].

As for the drag, we rely on the discussion of [18], which provides also extensive description of experimental results confirming theoretical predictions. In the case of symmetric heating a steady, convection state with $v_s \neq 0$ exists, is stable and the amplitude of all perturbations goes exponentially to zero without any oscillation whenever:

$$\alpha_E \equiv \frac{f_W}{2\rho_0 c_p h_W} < 2 \tag{10}$$

and, simultaneously,

$$\beta_E \equiv \frac{ag}{f_W\left(\frac{\Delta s}{\pi}\right)}\left(\frac{\rho_0 c_p}{h_W}\right)^2 R_1\left(\frac{1+\frac{L-2\Delta s}{\Delta s}}{1+\frac{L-2\Delta s}{2\Delta s}}\right) > 1 \tag{11}$$

where $f_W \equiv \frac{2|\boldsymbol{F}|}{\rho_0 v_s} = 2R$, R_1 is the first coefficient of the cosine-Fourier series in the angle $\varphi = \frac{\pi s}{\Delta s}$ of the quantity $\frac{h_W T_0(s)}{\rho_0 c_p} + q_W(s)$ in the case $\Delta s = \frac{L}{2}$, $q_W(s)$ is the heat produced by dissipative processes per unit time and unit volume of fluid and $\left(\frac{1+\frac{L-2\Delta s}{\Delta s}}{1+\frac{L-2\Delta s}{2\Delta s}}\right)$ is a corrective multiplicative factor which takes into account that $\Delta s \le \frac{L}{2}$ and reduces to 1 (to 2) if $\Delta s \to \frac{L}{2}$ $\left(\Delta s << \frac{L}{2}\right)$. (Here we refer to equations (2), (3), (4), (5), (16) and to the discussions of pages 491 and 500 of [18], where the quantities α_E and β_E are referred to as α and β respectively). If we neglect bulk heating - as in our equation (6) above - then we may neglect $q_W(s)$. Furthermore, if we take the same $T_0(s)$ of [17] (namely, $T_0(s) = T_0(s = 0)$, $T_0(s) = T_0(s = 0) - \Delta\Theta$ in the bottom and in the top arc-like section respectively) then:

$$R_1 = \frac{2h_W \Delta\Theta}{\pi\rho_0 c_p} \tag{12}$$

(Here we refer to Table D-1 and Sec. 4-11-16 of [24]). Together, (7), (8), (10) and $f_W = 2R$ give:

$$\alpha_E = \frac{R}{k} \tag{13}$$

i.e., α_E plays the role of a modified Prandtl number, being the ratio of the inverse drag-relevant timescale and the inverse timescale relevant to heat conduction between the fluid and the wall of the tube. Physically, small values of a correspond to an extremely good heat transfer at the fluid/wall interface. If $\alpha_E < 2$ any temperature disturbance is immediately suppressed. This prevents feedback of such temperature disturbances after one cycle (as in [17] and [19]) and leads to exponentially decreasing disturbance amplitudes [18]. To grasp the physical mechanism of instability at large α_E, let us quote [17]: *a warm pocket of fluid* (undergoes a stronger buoyancy. Then, it) *creates maximum flow rate going through the upper part and minimum flow rate going through the lower part of the loop. Accordingly, it passes quicker through the heat sink than through the heat source, and the latter becomes more effective. Similarly, the heat sink acts more effectively on a cold pocket of fluid*. A good heat transfer between the fluid and the wall prevents the formation of warm pockets and tends therefore to suppress this instability - see also Sec. 5.8.11 of [25]. Finally, for $\Delta s << \frac{L}{2}$ equations (7), (8), (11), (12) and $f_W = 2R$ give:

$$\beta_E = \frac{2\alpha g \Delta\Theta}{Rk\Delta s} \tag{14}$$

This parameter is proportional to the forcing temperature difference $\Delta\Theta$ and comparable to the Rayleigh number in the Bénard convection problem; it is basically the ratio of buoyancy and drag forces (The factor 2 is the multiplicative factor which corresponds to $\Delta s << \frac{L}{2}$). As anticipated, convection starts as $\beta_E > 1$; thus, (11) and (10) are the conditions for the existence and the stability of the steady convective state respectively. Both depend crucially on k and R. The former is described by (8). We need information on the latter.

4. Drag

The drag force $\rho_0 RLAv_s$ does an amount:

$$W = \rho_0 RLAv_s^2 \tag{15}$$

of mechanical work per unit time on the fluid. Both in [17] and [18] viscosity is referred to only vaguely; indeed, their discussion relies on no detailed description of the physical process underlying the drag. In the words of [17] *the present stability problem does not change qualitatively in the more general case*. We take advantage of this fact below.

If the external world applies no magnetic field, then the drag is only due to viscosity (formally, we write $R = R_{visc}$). In this case, W is just equal to the amount $W_{visc} = (\rho_0 R_{visc} LAv_s) \cdot v_s$ of heat produced by viscosity per unit time in the fluid. The explicit expression of R_{visc} depends on the detailed description of viscous losses, which in turn depends usually on the actual value of v_s. According to (4), we identify the friction with the wall as the main source of viscous drag. Moreover, if we identify the total amount $W_{visc} \cdot t_{loop} = (\rho_0 R_{visc} LAv_s) \cdot v_s \cdot \frac{L}{v_s}$ of energy dissipated by viscosity in the time t_{loop} with the product of the total fluid volume $L \cdot A$ and an equivalent pressure drop $\Delta H = \frac{f_D L \rho_0 v_s^2}{2D}$ (f_D Darcy factor) then we obtain $\rho_0 \cdot R_{visc} \cdot L \cdot A \cdot v_s \cdot v_s \cdot \frac{1}{v_s} = L \cdot A \cdot f_D \cdot L \cdot \rho_0 \cdot v_s^2 \cdot \frac{1}{2D}$, hence $\rho_0 R_{visc} v_s = \Delta H$, i.e.:

$$R_{visc} = \frac{f_D v_s}{2D} \tag{16}$$

Where - according to Colebrook-White equation - f_D depends on both $D = 2R_0$, Re and the wall roughness. We anticipate that in real-life applications Reynolds number satisfies:

$$Re > 2{,}300 \tag{17}$$

and in this case we write:

$$f_D = f_N \cdot Re^{-1/2} \;;\; f_N = 0.3164 \tag{18}$$

Let us apply a constant and uniform magnetic field $\boldsymbol{B}$ perpendicular to the direction of the flow: $\boldsymbol{B} \cdot \boldsymbol{s} = 0$. If the fluid has a scalar electrical conductivity σ such that the magnetic Reynolds number $Re_m \equiv \mu_0 \sigma v_s R_0$ ($\mu_0 = 4\pi \cdot 10^{-7}\ T \cdot m \cdot A^{-1}$ magnetic permittivity of vacuum) satisfies:

$$Re_m << 1 \tag{19}$$

then a Lorenz force with volume density $\boldsymbol{j} \wedge \boldsymbol{B}$ acts on the fluid, where $\boldsymbol{j} = \sigma\, \boldsymbol{v} \wedge \boldsymbol{B}$ is the density of an electric current which can be collected on the tube walls [8]. Inequality (19) means that the fluid motion leaves the magnetic field lines unaffected - see Sec. 66 of [26]; $\boldsymbol{j}$ is constant in steady state, then we speak of DC current. The Lorenz force acts on the fluid as a further drag with intensity $\sigma |\boldsymbol{B}|^2 v_s$ on the fluid and adds to $\boldsymbol{F}$, so that:

$$R = R_{visc} + R_{Lorenz}$$

$$R_{Lorenz} \equiv \frac{\sigma \mid \boldsymbol{B} \mid^2}{\rho_0} \tag{20}$$

$$W = W_{visc} + W_{Lorenz}$$

Inequalities (17) and (19) play the role of self-consistency conditions for the description of the drag provided by (16) and (20).

Apart from that, we stress again the crucial point that the results of both [17] and [18] invoked so far do not depend on the detailed nature of the drag; we may therefore apply them to the case where both viscous and magnetic drag occur. In contrast with R_{visc}, R_{Lorenz} does not depend on v_s. Moreover, the quantities $W_{visc} = \rho_0 R_{visc} L A v_s^2$ and $W_{Lorenz} = (\rho_0 R_{Lorenz} L A v_s) \cdot v_s = |\boldsymbol{B}|^2 L A v_s^2$ are the amount of work spent by the fluid per unit time in order to overcome the viscous and the Lorenz drag respectively. We may further split $W_{Lorenz} = W_{Joule} + W_{grid}$, where W_{Joule} is the amount of heat dissipated per unit time in the fluid through Joule heating and W_{grid} is the DC electric power actually picked up at the tube walls, which can be made available to the electric grid. The actual partition between W_{Joule} and W_{grid} depend on the external electric impedances the tube walls are connected to. Under optimal impedance matching:

$$W_{grid} = W_{Joule} = \frac{W_{Lorenz}}{2} = \frac{\sigma \mid \boldsymbol{B} \mid^2 L A v_s^2}{2} \tag{21}$$

for the maximum power transfer theorem. Let us introduce the dimensionless quantity $H \equiv \frac{W_{Lorenz}}{W_{visc}} = \frac{R_{Lorenz}}{R_{visc}}$. It is equal to the ratio of Lorenz and viscous force; should $R_{visc}^{-1} = \nu^{-1} R_0^2$ as for the viscous damping timescale in Newtonian fluids where viscous dissipation is ruled by bulk effects rather than by interactions with the wall, H would just reduce to the squared Hartmann number of MHD [8]; we may therefore say that H is a modified squared Hartmann number. Relationships (20) and (21) give then:

$$R = \frac{H+1}{H} \frac{\sigma \mid \boldsymbol{B} \mid^2}{\rho_0} \tag{22}$$

and

$$W \equiv 2 \frac{H+1}{H} W_{grid} \tag{23}$$

if $\sigma|\boldsymbol{B}|^2 \to 0$ (i.e., either the fluid is an electrical insulator or the magnetic field is too weak) then $H \to 0$ and viscous processes rule the drag. In contrast, if $\sigma|\boldsymbol{B}|^2$ is large enough, then $H >> 1$ and the drag is basically of magnetic origin. In this case, (23) tells us that basically one half of the amount W of work spent per unit time by the fluid to overcome the drag and keep on moving along the tube is converted into useful electric power W_{grid}. Since steady convection is driven by a constant $\Delta\Theta$, this is equivalent to direct conversion of thermal into electric power.

5. Useful formulas

It is possible to write both $|\boldsymbol{B}|$, v_s and $\Delta\Theta$ as functions of α_E and β_E. Together, (13), (20) and (22) give:

$$|\boldsymbol{B}| = \sqrt{\frac{H}{H+1}\frac{\rho_0 k}{\sigma}\alpha_E} \tag{24}$$

Together, (13), (16), (18), (20), (22) and the definitions of D, H, Re and v give:

$$v_s = \left(\frac{4}{f_N}\frac{1}{H+1}\right)^2 \frac{\rho_0}{\mu} R_0^{\,3} k^2 \alpha_E^{\,2} \tag{25}$$

Together, (9), (14), (16), (18), (20), (25) and the definitions of D, H, Re and β_E give:

$$\Delta\Theta = 8\left(\frac{1}{f_N}\frac{1}{H+1}\right)^2 \frac{\rho_0}{\mu}\frac{R_0^{\,3}k^3}{ag}\alpha_E^{\,3}\beta_E \tag{26}$$

Together with equation (8), equations (24)-(26) are useful because they allow us to rewrite $|\boldsymbol{B}|$, v_s and $\Delta\Theta$ in terms of quantities of practical interest for a system with given geometry (R_0, L, Δs...) and required working conditions ($\Delta\Theta$, W_{grid}) with a fluid with known physical properties (ρ_0, σ, α...) - precisely through α_E and β_E. Together, indeed, (9), (24), (25) and the definitions of A and W_{grid} give:

$$H = \frac{8}{\pi f_N}\left(\frac{R_0}{\Delta s}\right)^{5/2}\left(\frac{\rho_0 R_0^{\,2} k}{\mu}\right)^{1/2}\left(\frac{W_{grid}}{\rho_0 R_0^{\,4} L k^3}\right) \tag{27}$$

where $W_{grid} \propto H$, in agreement with (21) and the definition of H. Moreover, (9), (25) and (27) give:

$$\alpha_E = \frac{8}{\pi}\left(\frac{H+1}{H}\right)\left(\frac{R_0}{\Delta s}\right)^2\left(\frac{W_{grid}}{\rho_0 R_0^{\,4} L k^3}\right) \tag{28}$$

where (27) ensures that $\alpha_E \propto \frac{W_{grid}}{H} < \infty$ at all values of H. Substitution of (27)-(28) in (24)-(25) provides us with the values of $|\boldsymbol{B}|$ and v_s (hence the mass flow) for a system with given geometry and a given working fluid, which we want to deliver a DC electric power W_{grid} to the grid. Furthermore, it must be checked that the value of v_s satisfy the self-consistency conditions (17) and (19). Finally, we rewrite (26) as follows:

$$\beta_E = \frac{\Delta\Theta}{\Delta\Theta_c} \;;\; \Delta\Theta_c = 8\left(\frac{1}{f_N}\frac{1}{H+1}\right)^2 \frac{\rho_0}{\mu}\frac{R_0^{\,3}k^3}{\alpha g}\alpha_E^{\,3} \tag{29}$$

Together, (28) and (29) provide both conditions (10) and (11) of existence and stability of a steady operation configuration with a simple meaning. Firstly, (10) and (29) mean that convection requires that the temperature jump $\Delta\Theta$ is larger than a minimum value. Secondly, if H is too low then of course η is too small, as no Lorenz force acts on the fluid. Finally, $\alpha_E^{\,3} \propto (H+1)^3$ and $\Delta\Theta \propto H+1$; if follows that if H becomes too large then $\Delta\Theta_c$ too increases until $\beta_E < 1$, (11) is violated and convection is suppressed; if we raise $|\boldsymbol{B}|$ to raise W_{grid} then $|\boldsymbol{B}|$ just chokes the flow as the magnetic drag is too strong. In other words, a magnetic field which is too strong stops convection; if it is too weak, no electric energy is obtained. Analogously, (11) and (28) imply that in stable conditions W_{grid} cannot be larger than an upper threshold, which in turn increases with L.

6. Efficiency

The efficiency of conversion of thermal power into electric power is $\eta \equiv \frac{W_{grid}}{W_{th}}$ where $W_{th} = \int dW_{th}$ is the amount of heat supplied by the external world to the fluid across the lateral surface of the tube in the arc-like connection at the bottom (and the domain of integration corresponds to this arc). Now, in the approximation of negligible heating of the fluid bulk underlying (6) and (12) W is negligible. Then, the amount of heat $W_{th} - W$ which goes from the fluid to the external world across the lateral surface in the arc-like connection at the top is $\approx W_{th}$ and (20), (21) and (23) imply that W_{grid} is also negligible. This approximation is therefore pessimistic, and provides just a lower bound $\eta_L < \eta$ on η. Accurate estimates of η require full description of the fluid heat balance in the vertical branches, including radiative cooling through the walls of the tube as well as both viscous and Joule heating. At given W_{grid}, moreover, underestimating η is equivalent to overestimate W_{grid} hence v_s (via (21)); thus, (9) provides us with an upper bound $v_M > v_s$.

However, together with the assumption of vanishing k along both left and right vertical branch of the loop our approximation ensures that the only source and the only pit of heat in the fluid is the thermal interaction with the external world through the walls of both top and bottom arc-like connections. As such, it implies that the maximum value of T is attained by the fluid at the exit of the bottom arc-like connection, and that this value is also equal to the value of T at the entry in the top arc-like connection, and vice versa for minimum value of T. Broadly speaking, the smaller W, moreover, the smaller W_{visc}, the smaller $v_s \propto \sqrt{W_{visc}}$ the larger $\left|\frac{\partial T}{\partial s}\right|$ in (6), the more effective the heat exchange with the wall, the nearer the difference of the values of T at the exit and the entry of the bottom arc-like connection to its maximum attainable value $\Delta\Theta$, the more accurate the following simple result:

$$W_{th} = \int dW_{th} = \int \rho_0 c_p \frac{dT}{dt} A ds = \int \rho_0 c_p A \frac{ds}{dt} dT = \rho_0 c_p A v_s \int dT = \rho_0 c_p A v_s \Delta\Theta \tag{30}$$

Together, (9), (14), (15), (23), (30) and the definition of η give the following lower bound on η:

$$\eta_L = \frac{1}{2} \frac{H}{H+1} \frac{Lag}{\beta_E} \tag{31}$$

According to (11) and (31), an obvious way to raise η_L for a fluid with α given is to raise L, as $0 \le \frac{H}{H+1} \le 1$. Of course, η_L never exceeds 1 even at large L; but then, at large L is is impossible to neglect $W \propto L$, and the approximation of negligible heating underlying (31) breaks down. Moreover, L must be large enough to satisfy the self-consistency condition (4). We may achieve large values of L by taking advantage of the fact that our results do not require that the vertical branches of our loop are vertical straight lines. Indeed, if we replace each straight vertical branches of Figure 1 with a vertical helix with pitch $\mathrm{H} \ge D$, height V and radius r - see Figure 2 - then the length of each branch is $\frac{V-D}{\mathrm{H}}\sqrt{\mathrm{H}^2 + 2\pi r^2}$, the total length of the loop is $L = 2\frac{V-D}{\mathrm{H}}\sqrt{\mathrm{H}^2 + 2\pi r^2} + 2\Delta s \approx 2\frac{V}{\mathrm{H}}\sqrt{\mathrm{H}^2 + 2\pi r^2} + 2\Delta s$ for $V >> D$, and as a whole the loop resembles a DNA molecule. We retrieve the vertical straight branches of Figure 1 in the $r << \frac{\mathrm{H}}{2\pi}$ limit, with $\frac{L}{2} = V$ vertical dimension. In contrast, if $r >> \frac{\mathrm{H}}{2\pi}$ then $L \approx 2V \cdot \frac{2\pi r}{\mathrm{H}}$, which in turn is maximized as $\mathrm{H} = D$:

$$L = \frac{4\pi V r}{D} = \frac{2\pi V r}{R_0} \tag{32}$$

so that L may be >> $2V$. If $\frac{V}{R_0}$ is large enough, L can attain huge values. We can assembly many helices together just by braiding them as H ≥ D. More simply, we can also assemble the ascending and the descending helix of each loop parallel to each other to form a closed loop where the fluid continually flows (see the caption of Figure 2 for the meaning of 'ascending' and 'descending' here). The helices can be oriented either clockwise, or both counterclockwise, or like in a DNA molecule (one clockwise, the other counterclockwise).

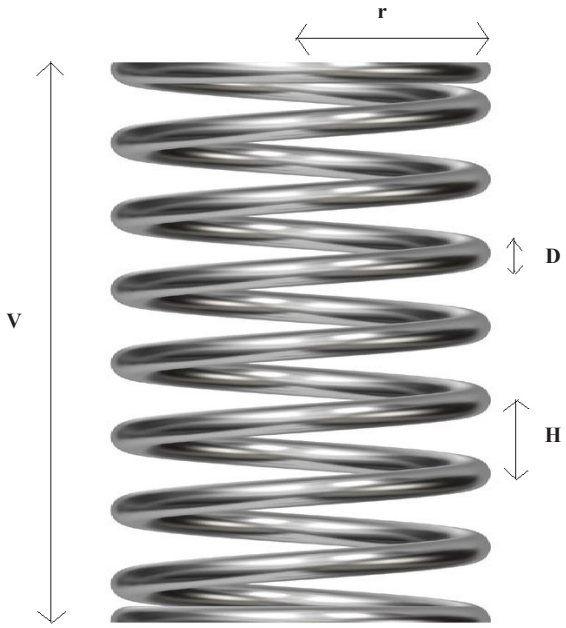

Figure 2. The helicoidal shape of one vertical branch. This shape may replace the vertical straight shape of a vertical branch (say, $\frac{\Delta s}{2} < s < \frac{L}{2} - \frac{\Delta s}{2}$) of Figure 1 and reduces to it as $r \to 0$. The pitch H cannot be shorter than D. Here we replaced the two vertical branches of the loop in Figure 1 with two twin helices, like a DNA molecule, with the fluid flowing upwards along one ('ascending') helix and downwards along the other ('descending') helix. Two arc-like connections with length Δs (not displayed here) connect the two helices at the top and at the bottom. Here V plays the role of the length $L = -\frac{\Delta s}{2}$ of one straight vertical branch of Figure 1. The fluid flows all along the closed loop formed by the ascending helix, the top connection, the descending helix and the connection at the bottom. Coaxial helices are also feasible

7. An example

To fix the ideas, we may think of a chimney that allows the environmentally safe escape of exhaust gases away from a furnace. The chimney can sustain both ascending and descending helices which are fixed to it and wrap it. The furnace provides the heating at the bottom, and radiative cooling occurs either at the top or - more realistically - all along the helices. In this lay-out r is basically the radius of the flue and V is the height of the chimney. (To break the symmetry and prevent the fluid from going on following both helices they can be located slightly asymmetrically with respect to the furnace). Along the helices, permanent magnets locally provide the required magnetic field. Once a fluid with suitable physical properties (including α and σ) is available, the system provides a cheap conversion of the thermal energy which would otherwise be lost per unit of time through the chimney into useful electric energy, thus allowing recovery of energy and reducing fuel consumption with no need of water, no moving parts and negligible maintenance issues.

Let us come up with some numbers. We work with a tube whose hydraulic diameter and its arc-like connection are D = 0.02 m and Δs = 1 m respectively. The tube forms a closed loop made of an ascending helix, a descending helix and two arc-like connections. Both helices have a pitch D and wrap a chimney with V = 30 m and r = 3 m. The tube is filled

with Galinstan™, a commercially available, atoxic, liquid metal alloy which remains in the liquid state between 254 K and 1,573 K at atmospheric pressure and leaves no solid residue when conducting an electric current. Its properties are listed in Table 1. We assume that the difference between the temperature at the bottom - i.e., near the furnace - and the temperature of the external environment which the fluid is thermally coupled to in the top arc-like connection is $\Delta\Theta$ = 350 K. Permanent magnets are located along the tube to provide a magnetic field perpendicular to the tube.

We want to obtain an electric power W_{grid} = 2,000 W. We ask ourselves if steady convection occurs, if it is stable (i.e., if both (10) and (11) are satisfied) and - in case - we ask ourselves how large are the required intensity of the magnetic field and if all self-consistency conditions (4), (17) and (19) are satisfied. We want also both the upper bound on the fluid speed along the tube and the lower bound on the efficiency.

Equations (9), (24), (27), (28), (29), (31) and (32) and the definitions of Re and Re_m give $\alpha_E = 0.426$, $\beta_E = 1.043$, $H = 5.007$, $Re = 1.239 \cdot 10^4$, $Re_m = 0.02$, $L = 5.655 \cdot 10^4$ m, $|\boldsymbol{B}| = 0.017$ T, $v_M = 0.462 \frac{m}{s}$, and $\eta_L = 2.1\%$.

Some final remarks. Both (4), (10), (11), (17) and (19) are satisfied, hence steady state conversion of thermal into electric power is feasible. Even in our far-from-optimized, back-of-the-envelope analysis the lower bound on efficiency is near to the values of TE [2, 3] and TA [6] conversion. Moreover, the intensity of the required magnetic field is fully compatible with the utilization of permanent magnets applied directly to the tube, and no external power supply is required. Local values ($= v_s \mid \boldsymbol{B} \mid \leq v_M \mid \boldsymbol{B} \mid = 7.6 \cdot 10^{-3} \frac{V}{m}$) of the electric field are scarcely dangerous. Furthermore, no solid residues (e.g., no salt deposit) affect the flow as no electrolysis occurs in Galinstan™. Furthermore the total mass of Galinstan™ involved ($\approx 1 \cdot 10^5$ Kg) is constant, needs no refilling, flows and produces electric power continuously 24/7 and is much less than the mass of the chimney ($\approx 5 \cdot 10^5$ Kg for a 30-m-high cylindrical corona with outer radius 3 m and thickness 0.5 m, made of bricks with specific weight 2,000 Kg/m^3); accordingly, installation on existing chimneys should raise no relevant problem. Finally, our estimate holds just on a back-of-the-envelope, over-conservative basis. Less pessimistic estimates of efficiency shall be the outcome of more accurate, numerical, future simulations.

Table 1. Properties of Galinstan™

Properties of Galinstan™		
ρ_0	$6.44 \cdot 10^3$	$Kg \cdot m^{-3}$
c_p	$2.96 \cdot 10^2$	$J \cdot Kg^{-1} \cdot K^{-1}$
h	$4.40 \cdot 10^3$	$W \cdot m^{-2} \cdot K^{-1}$
α	$1.83 \cdot 10^{-5}$	K^{-1}
κ	$1.65 \cdot 10^{-1}$	$W \cdot m^{-1} \cdot K^{-1}$
μ	$2.40 \cdot 10^{-3}$	$Kg \cdot m^{-1} \cdot K^{-1}$
σ	$3.46 \cdot 10^6$	$S \cdot m^{-1}$

We refer to both Table 1 of [27] and Table 4 of [28]. As for α, we take the value for Ga. As for h, values in the range $4.40 \cdot 10^3 \leq h \leq 7 \cdot 10^4$ $W \cdot m^{-2} \cdot K^{-1}$ are reported; conservatively, we took the lowest value. The resulting value of Pr is 4.305
Remarkably, σ is about 3 times larger and 7 orders of magnitude larger than the corresponding values for Hg and ferrofluids (0.1 $S \cdot m^{-1}$) [16] respectively

8. Conclusions

As a novel approach to waste heat recovery, we have investigated the convection of an electrically conducting, viscous, incompressible, single-phase fluid in a tube with the constant hydraulic diameter and shaped as a vertical closed loop, which the external world applies a temperature difference to. We invoke the model of [17] and its extension

discussed in [18]. For a given distribution of temperature of the wall of the tube, in this model:

(a) the motion of the fluid is ruled by both the buoyancy force and the drag force exerted by the wall of the tube on the fluid.

(b) heat conduction between the fluid and the wall of the tube is the only process ruling both the heating and cooling of the fluid.

If the wall is kept warmer at the bottom than at the top (i.e., if the external world applies a suitable temperature gradient to the loop) then convection is possible. In a steady state, the same amount of heat flows per unit time from the external world into the fluid and vice versa through the wall of the arc-like connection at the bottom and at the top respectively. We adopt the familiar Boussinesq approximation. Moreover, the temperature of the fluid is uniform over each cross-section of the tube, as the timescale of both momentum diffusion and heat conduction across each cross-section is much shorter than the time required for a complete turn around the loop. Accordingly, the fluid motion is basically 1D, directed along the tube.

The model predicts that the flow rate and the Reynolds number increase with increasing heat flux, and that the Nusselt number is basically uniform along the loop. These predictions agree with the results of the experiments of [21-23] respectively. Experiments [18] also confirm two further predictions: convection with constant fluid velocity starts as buoyancy overcomes the drag and remains stable whenever good heat transfer at the fluid/wall interface suppresses instabilities.

Even if experiments have been carried out with no magnetic field so far - i.e., with a purely viscous drag exerted on the fluid, so that the electric conductivity σ of the latter plays no role - the model relies on no detailed description of the physical nature of the drag. We take advantage of this fact; the novelty of this work is the inclusion of a magnetic field in the model. If a magnetic field is applied, then it exerts a Lorenz force on the electrically conducting fluid. A Lorenz force acts as a drag in analogy with the viscous drag. In contrast with thermomagnetic convection [10], which is relevant to the research on ferrofluids and where the magnetic force acting on the fluid depends on the gradients of magnetization and of a magnetic field [11], here the drag is proportional to σ. The additional drag due to the Lorenz force induces additional dissipation of power in the fluid. The interaction of the magnetic field with the moving, electrically conducting fluid produces an electric current. If the magnetic field is directed perpendicularly to the fluid flow, the electric current may be picked up at the wall and provide the power grid in the external world with DC electric power. Such power is proportional to the power dissipated in the fluid (which in turn is proportional to the squared fluid velocity) and is obtained at the expense of the mechanical power of the convective motion of the fluid, which in turn is driven by the externally applied temperature gradient. Conversion of heat into electricity follows. Since the tube cross-section is uniform along the loop, both the fluid velocity and the density of collected electric power are also uniform along the loop.

Both the actual existence and the stability of this conversion in a steady state are described by the model of [17, 18] with a suitable description of the total (viscous + Lorenz) drag. The model computes also both the required magnetic field and temperature difference, as well as the resulting fluid velocity, for a loop of given geometry filled with a known fluid to deliver a known amount of electric power to the grid.

Physically, convection starts when buoyancy overcomes the drag. The latter may include both a viscous drag and (if the magnetic field is $\neq 0$) a magnetic drag. The latter induces in the moving, electrically conducting fluid an electric field, which in turn drives an electric current flowing perpendicularly to the flow. The latter can be picked up at the wall of the tube, the related electric power is obtained at the expense of the mechanical power of the fluid - then, eventually, of the amount of heat that flows from the hottest to the coldest point of the loop.

However, convection may be unstable. A steady convection state (which can deliver a constant electric power) is destabilized if the heat transfer at the fluid/wall interface is poor. In this case, indeed, if a perturbation of temperature leads to the formation of a warm pocket of fluid, then the latter undergoes a stronger buoyancy. Thus, it creates a maximum flow rate going through the upper part and a minimum flow rate going through the lower part of the loop. Accordingly, it passes quicker through the heat sink than through the heat source, and the latter becomes more effective. Similarly, the heat sink acts more effectively on a cold pocket of fluid. A good heat transfer between the fluid and the wall prevents the formation of warm pockets and tends therefore to suppress this instability [17, 25].

When it comes to computing the efficiency of this conversion, admittedly, the model is over-pessimistic, as its tenet of the heat exchange with the wall being the only source of heat for the fluid just makes us neglect the Joule heating of

the fluid bulk which is intertwined with the production of electricity. Thus, the model can only estimate a lower bound on the efficiency.

Given the DC power to the grid, moreover, underestimating the efficiency is equivalent to overestimating the amount of heat to be converted per unit of time which is carried by the fluid from the hotter bottom to the colder top of the loop, an amount which is proportional to the velocity of the fluid. The model provides therefore just an upper bound on this velocity.

It turns out that the lower bound on the efficiency increases with both increasing σ and increasing total length of the loop. To fix the ideas and figure out what the relevant orders of magnitude are like, we take advantage of the fact that the model of [17, 18] describes convection just as a 1D motion along the tube and makes no assumption concerning the overall shape of the loop, as far as the fluid is free to go up and down between a hotter section at the bottom and a colder section on the top of the loop. To obtain a very long, closed loop we imagine a 1-cm radius tube that forms two coaxial helices with a 3 m radius, 2-cm pitch and 30 m vertical size connected at the top and the bottom to form a double-helix loop, much like the DNA molecule. We may locate such tall helices around an existing chimney, which allows the escape of exhaust gases away from a furnace. The chimney can sustain both helices which are fixed to it and wrap it. The furnace provides the heating at the bottom, the fluid goes up following one helix, gets colder at the top, or - more realistically - all along the helices through radiative cooling and goes down following the other helix. (To break the symmetry and prevent the fluid from going on following both helices they can be located slightly asymmetrically concerning the furnace). Permanent magnets are located along helices and provide the required magnetic field. As a working fluid, we choose Galinstan™, an atoxic, incompressible, single-phase liquid metal alloy with very large σ which leaves no solid residue.

We have shown that it is possible to obtain 2 KW DC electric power with no instability and with the help of a 350 K difference between the temperature at the bottom - i.e., near the furnace - and the temperature of the external environment which Galinstan™ is thermally coupled to at the top of the loop (the temperature gradient is $\frac{350}{30} = 11.67 \frac{K}{m}$). For this purpose, we need a 0.017 T magnetic field, which is easily achievable by commercially available permanent magnets. The resulting lower bound on the conversion efficiency and upper bound on the fluid velocity are 2.1% and $0.462 \frac{m}{s}$ respectively.

As for efficiency, this result suggests that the system is competitive both with Thermoelectric (TE) [2] and Thermoacoustic (TA) [6] energy conversion systems for the same electric power and at atmospheric pressure. As for the velocity, low velocities imply low values of the density of the collected electric power. The low value of the latter, in turn, allows static conversion of energy, facilitates built-in prevention of unwanted overvoltage, parasitic arcs and overheating already from the drawing desk and ensures that once implementation with optimal impedance matching between the system and the external world has occurred this matching endures long operation undisturbed with no need of additional cooling systems (in contrast with TE). Moreover, a low value of fluid velocity corresponds to moderate intensity of the magnetic field (too-strong magnetic fields just suppress convection altogether, too-weak fields give poor conversion to electric energy). In turn, moderate intensity of the magnetic field strongly reduces mechanical stresses (in contrast with TA) - thus facilitating both assembly, operation and maintenance - and allows utilization of permanent magnets, the uniformity of the field lines being easily obtained through suitable localization of pole pieces and air gaps along the tube. The Lack of electromagnets and superconductors allows the system to operate with no need for external auxiliary, power supply systems. Finally, if the fluid velocity is low then, the magnetic Reynolds number [8] too is low. This means that the fluid does not perturb the field lines of the superimposed magnetic field; the latter can therefore be accurately designed from scratch.

In conclusion, if a moderate external temperature gradient is maintained, then the convection of liquid metal in a closed loop with a uniform magnetic field allows the conversion of heat into electricity which:

- needs no water supply.
- involves no gears and no moving solid parts altogether.
- is silent (unlike TA).
- is environmentally safe (the liquid always remains confined with the loop).
- works 24/7 continuously (unlike TE with photovoltaic cells).
- depends weakly on weather (unlike TE with photovoltaic cells).

- works at atmospheric pressure (unlike TA).
- allows easy maintenance (liquid losses due to possible leakage may easily be refilled).
- produces no solid residue (salt, and the like).
- involves no phase transition (Galinstan™ evaporates nowhere and freezes below -19 °C).
- requires no power supplies (permanent magnets only).
- has simple magnetic field geometry (unlike thermomagnetic convection).
- requires no active cooling system (unlike high power TE).
- has limited magneto-mechanical stress (low magnetic field unlike high power TA).
- has a conversion efficiency > 2.1% (competitive with TA at atmospheric pressure and TE).
- is compatible with existing industrial environment (as our example with the chimney shows).

More accurate estimates of the conversion efficiency, and discussion of the behaviour of the system at temperature < -19 °C (when Galinstan™ freezes, but overcooled liquid flow is still possible [29]) are the topic of future work.

Conflict of interest

The authors declare that they have no conflict of interest.

References

[1] Jouhara H, Khordehgah N, Almahmoud S, Delpech B, Chauhan A, Tassou SA. Waste heat recovery technologies and applications. *Thermal Science and Engineering Progress*. 2018; 6: 268-289.

[2] Comamala M, Pujol T, Ruiz Cózar I, Massaguer E, Massaguer A. Power and fuel economy of a radial automotive thermoelectric generator: Experimental and numerical studies. *Energies*. 2018; 11: 2710.

[3] Amine Zoui M, Bentouba S, Stocholm JG, Bourouis M A review on thermoelectric generators: Progress and applications. *Energies* 2020; 13: 3606.

[4] Alemany A, Carcangiu S, Forcinetti R, Montisci A, Roux JP. Feasibility analysis of an mhd inductive generator coupled with a thermoacoustic resonator. *Magnetohydrodynamics*. 2015; 51: 531-541.

[5] Alemany A, Krauze A, Al Radi M. Thermo acoustic - MHD electrical generator. *Energy Procedia.* 2011; 6: 92-100.

[6] Swift GW. Thermoacoustic engines. *The Journal of the Acoustical Society of America*. 1988; 84(4): 1145-1180.

[7] Wu Z, Zhang L, Dai W, Luo E. Investigation on a 1 kW traveling wave thermoacoustic electrical generator. *Applied Energy*. 2014; 124: 140-147.

[8] Jackson JD. *Classical Electrodynamics*. New York: Wiley & Sons; 1962.

[9] Japikse D. Advances in thermosyphon technology. *Advances in Heat Transfer*. 1973; 9: 1-111.

[10] Finlayson BA. Convective instability of ferromagnetic fluids. *Journal of Fluid Mechanics*. 1970; 40(4): 753-767.

[11] Mukhopadhyay A, Ganguly R, Sen S, Puri IK. A scaling analysis to characterize thermomagnetic convection. *International Journal of Heat and Mass Transfer.* 2005; 48: 3485-3492.

[12] Manna NK, Nirmalendu C, Biswas N, Sarkar UK, Öztop HF, Abu-Hamdeh NH. Effect of multibanded magnetic field on convective heat transport in linearly heated porous systems filled with hybrid nanofluid. *Physics of Fluids*. 2021; 33: 053604.

[13] Manna NK, Mondal MK, Biswas N. A novel multi-banding application of magnetic field to convective transport system filled with porous medium and hybrid nanofluid. *Physica Scripta*. 2021; 96: 065001.

[14] Mandal DK, Mondal MK, Biswas N, Manna NK, Gorla RSR, Chamka AJ. Nanofluidic thermal - fluid transport in a split-driven porous system working under a magnetic environment. *International Journal of Numerical Methods for Heat & Fluid Flow*. 2022; 32(7): 2543-2569.

[15] Manna NK, Biswas N, Mandal DK., Sarkar UK, Öztop H, Abu-Hamdeh N. Impacts of heater-cooler position and Lorentz force on heat transfer and entropy generation of hybrid nanofluid convection in quarter-circular cavity. *International Journal of Numerical Methods for Heat & Fluid Flow.* 2023; 33(3): 1249-1286.

[16] Pant RP, Dhawan SK, Suri DK, Arora M, Gupta SK, Koneracka M, et al. Synthesis and characterization of ferrofluid-conducting polymer composite. *Indian Journal of Engineering and Materials Sciences*. 2004; 11: 267-270.

[17] Welander P. On the oscillatory instability of a differentially heated fluid loop. *Journal of Fluid Mechanics*. 1967;

29(1): 17-30.
[18] Erhard P, Mueller U. Dynamical behaviour of natural convection in a single-phase loop. *Journal of Fluid Mechanics*. 1990; 217: 487-518.
[19] Moore DW, Spiegel EA. A thermally excited non-linear oscillator. *Astrophysical Journal*. 1966; 143: 871-887.
[20] Keller JB. Periodic oscillations in a model of thermal convection. *Journal of Fluid Mechanics*. 1966; 26(3): 599-606.
[21] Asif M, Siddiqui MA. Heat transfer studies during natural convection of water and ethanol in a closed loop vertical-annular thermosyphon. Available from: https://www.researchgate.net/publication/301770361_Heat_Transfer_Studies_during_Natural_Convection_of_Water_and_Ethanol_in_a_closed_loop_Vertical-Annular_Thermosyphon [Accessed 22nd August 2023].
[22] Mustafa J, Husain S, Siddiqui MA. Experimental studies on natural convection of water in a closed loop vertical annulus. *Experimental Heat Transfer*. 2017; 30(1): 25-45.
[23] Husain S, Siddiqui MA. Experimental and numerical analyses of natural convection flow in a partially heated vertical annulus. *Numerical Heat Transfer, Part A: Applications*. 2016; 70(7): 763-775.
[24] Korn GA, Korn Th M. *Mathematical Handbook for Scientists and Engineers*. Chelmsford MA, USA: Courier Corporation; 2013.
[25] Di Vita A. *Non-Equilibrium Thermodynamics*. Berlin: Springer Nature; 2022.
[26] Landau LD, Lifschitz EM. *Electrodynamics of Continuous Media*. 2nd ed. Oxford, UK: Pergamon Press; 1984.
[27] Zhang XD. Experimental investigation of galinstan-based minichannel cooling for high heat flux and large heat power thermal management. *Energy Conversion and Management*. 2019; 185: 248-258.
[28] Liu S, Sweatman K, MacDonald S, Nogita K. Ga-based alloys in microelectronics interconnects: A review. *Materials*. 2018; 11: 1384-1404.
[29] Tang SY, Tabor Ch, Kalantar-Zadeh K, Dickey MD. Gallium liquid metal: The devil's elixir. *Annual Review of Materials Research*. 2021; 51: 381-408.